Inorganic Chemistry

Article

pubs.acs.org/IC

trans-[Ru^{II}(dpp)Cl_2]: A Convenient Reagent for the Preparation of Heteroleptic Ru(dpp) Complexes, Where dpp Is 2,9-Di(pyrid-2′-yl)-1,10-phenanthroline

Ruifa Zong, Bin Wang, and Randolph P. Thummel*

Department of Chemistry, 136 Fleming Building, University of Houston, Houston, Texas 77204-5003, United States

Supporting Information

ABSTRACT: The reaction of 2,9-di(pyrid-2′-yl)-1,10-phenanthroline (dpp) with [$RuCl_3$·$3H_2O$] or [$Ru(DMSO)_4Cl_2$] provides the reagent *trans*-[Ru^{II}(dpp)Cl_2] in yields of 98 and 89%, respectively. This reagent reacts with monodentate ligands L to replace the two axial chlorides, affording reasonable yields of a ruthenium(II) complex with dpp bound tetradentate in the equatorial plane. The photophysical and electrochemical properties of the tetradentate complexes are strongly influenced by the axial ligands with electron-donating character to stabilize the ruthenium(III) state, shifting the metal-to-ligand charge-transfer absorption to lower energy and decreasing the oxidation potential. When the precursor *trans*-[Ru^{II}(dpp)Cl_2] reacts with a bidentate (2,2′-bipyridine), tridentate (2,2′;6,2″-terpyridine), or tetradentate (itself) ligand, a peripheral pyridine on dpp is displaced such that dpp binds as a tridentate. This situation is illustrated by an X-ray analysis of [Ru(dpp)(bpy)Cl](PF_6).

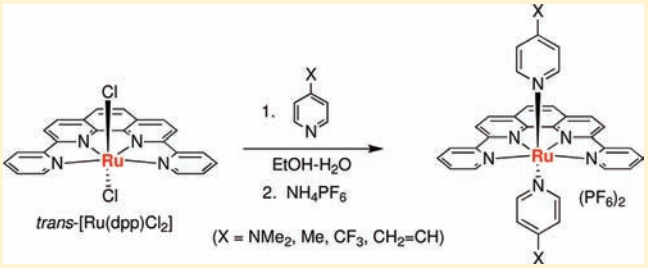

■ INTRODUCTION

Over the past several decades, the field of ruthenium polypyridine chemistry has experienced phenomenal growth. The mainstay ligands in this vast family of complexes are the bidentate 2,2′-bipyridine (bpy) and the tridentate 2,2′:6′,2″-terpyridine (tpy).[1] These ligands have been elaborated in almost every way imaginable including the replacement of H atoms with other groups, the substitution of other elements for C atoms in the pyridine rings, and the incorporation of aza-aromatic rings other than pyridine. Ruthenium(II) complexes of bpy and tpy have fundamental structural and photophysical differences. The tris-bidentate complex $[Ru(bpy)_3]^{2+}$ exists as a pair of enantiomers, while the bis-tridentate complex $[Ru(tpy)_2]^{2+}$ (**5**) is achiral. The bpy complex has a long excited-state lifetime (1100 ns)[2] and hence very rich photophysical chemistry, while the tpy complex, being more highly strained because of the two fused five-membered chelate rings, has a much shorter lifetime (0.3 ns)[3] and thus a somewhat more limited range of useful photophysics.[4]

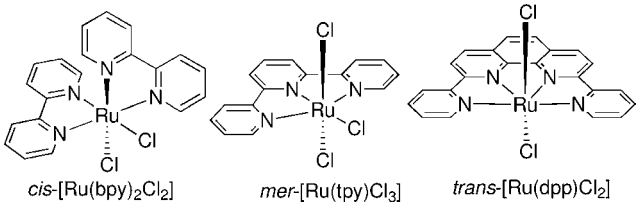

Recently, we prepared a new ligand in this series, 2,9-di(pyrid-2′-yl)-1,10-phenanthroline (dpp).[5,6] The central phenanthroline ring restricts the conformational freedom of the ligand and thus prevents it from binding as a bis-bidentate bridging ligand. Instead, all four pyridines bind to Ru^{II} to form surprisingly stable tetradentate complexes that can accommodate two monodentate ligands in the remaining axial positions (**1a**−**1h**). One of the interesting properties of these Ru^{II}(dpp) complexes is that they all appear to be active water oxidation catalysts, and we are carrying out a thorough investigation of this important feature.

In our initial reports on these dpp complexes, we prepare them in a "one-pot" synthesis, wherein dpp is treated with [$RuCl_3$·$3H_2O$] in aqueous ethanol (EtOH), followed by the addition of excess monodentate ligand and triethylamine to complete the coordination sphere. In this process, some dpp binds as a tridentate, and thus $[Ru(dpp)_2]^{2+}$ is formed as a byproduct. In this report, we isolate and characterize the intermediate *trans*-[Ru^{II}(dpp)Cl_2], study its reaction with various ligands, and explore the novel Ru^{II}(dpp-*N*,*N*′,*N*″) complexes, where dpp binds to the metal in a tridentate fashion.

■ RESULTS AND DISCUSSION

Synthesis and Characterization. *trans*-[Ru^{II}(dpp)Cl_2] was prepared by two different methods. The reaction of dpp and an equimolar amount of [$RuCl_3$·$3H_2O$] in EtOH gave the complex, often with some unreacted dpp, depending on the quality of the highly hygroscopic [$RuCl_3$·$3H_2O$]. We found that quickly adding dpp into an ethanolic solution of excess

Received: December 8, 2011
Published: February 10, 2012

   dx.doi.org/10.1021/ic202648h | *Inorg. Chem.* 2012, 51, 3179−3185

$[RuCl_3{\cdot}3H_2O]$, after refluxing overnight, gave a 98% yield of *trans*-$[Ru^{II}(dpp)Cl_2]$ as a dark-green solid. The complex is obtained in its pure form, as suggested by its ^1H NMR spectrum after being washed thoroughly with EtOH and acetone and dried. However, contamination by the excess $[RuCl_3{\cdot}3H_2O]$ could not be excluded. An alternative synthesis of *trans*-$[Ru^{II}(dpp)Cl_2]$ in 89% yield is to treat dpp with 1 equiv of $[Ru(DMSO)_4Cl_2]$ in refluxing $CHCl_3$. The precipitate was collected, washed with $CHCl_3$ and acetone, and dried. A positive matrix-assisted laser desorption ionization time-of-flight (MALDI-TOF) analysis of *trans*-$[Ru^{II}(dpp)Cl_2]$ using a mixture of CH_2Cl_2 and MeOH for the sample loading revealed peaks at m/z 506.3, 471.3, and 436.4 corresponding to $[M]^+$, $[M - Cl]^+$, and $[M - 2Cl]^+$, respectively. The purity of the material prepared by the second method was further confirmed by its ^1H NMR spectrum and elemental analysis. Similar to *cis*-$[Ru(bpy)_2Cl_2]$ and *mer*-$[Ru(tpy)Cl_3]$, the neutral complex *trans*-$[Ru^{II}(dpp)Cl_2]$ is not very soluble in solvents other than *N*,*N*-dimethylformamide (DMF) and dimethyl sulfoxide (DMSO). In DMSO-d_6, a freshly prepared sample showed a complicated spectrum of two or more species. The color of the NMR solution changed from dark to light brown, indicating the likely replacement of chloride by a solvent molecule. After standing overnight, a DMSO-d_6 solution of *trans*-$[Ru^{II}(dpp)Cl_2]$ showed only seven ^1H NMR signals, consistent with its trans structure and tetradentate dpp binding. It is not clear if one or two Cl atoms were replaced.

As opposed to the one-pot synthesis of dpp complexes, the use of isolated *trans*-$[Ru^{II}(dpp)Cl_2]$ resulted in higher yields for weaker monodentate ligand systems and less complicated product distribution (Scheme 1). In our previous report, using

Scheme 1. Synthesis of *trans*-$[Ru^{II}(dpp)Cl_2]$

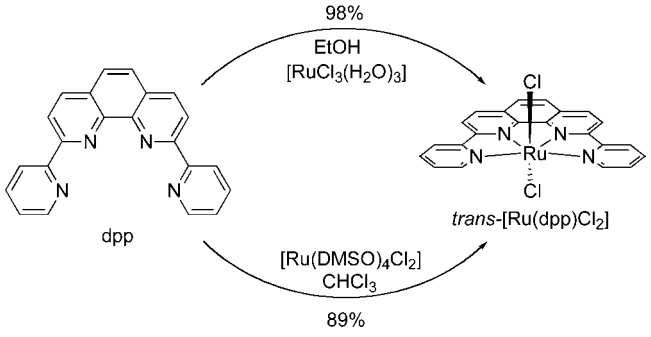

the one-pot approach, *trans*-$[Ru(dpp)(4\text{-}CF_3\text{-}py)_2]^{2+}$ (**1c**) was prepared in only 5% yield, while the major product (52%) was *trans*-$[Ru(dpp)(4\text{-}CF_3\text{-}py)Cl]^+$. We found that the yields changed to 44% and 22% for the bispyridine and monopyridine complexes, respectively, when isolated *trans*-$[Ru^{II}(dpp)Cl_2]$ was used for their preparation. It is noteworthy that no bis-dpp complex $[Ru(dpp)_2]^{2+}$ (**2**) was produced under these conditions.

Similar to the synthesis of complexes **1a**–**1c**, 4-vinylpyridine (VP) reacts with *trans*-$[Ru^{II}(dpp)Cl_2]$ to afford a quantitative yield of *trans*-$[Ru^{II}(dpp)(VP)_2](PF_6)_2$ (**1d**; Scheme 2). The VP protons exhibit a AA′XX′ pattern, and the vinyl protons show stronger trans coupling (17.86 Hz) than cis coupling (10.99 Hz), whereas no geminal coupling was detected. Treatment of *trans*-$[Ru^{II}(dpp)Cl_2]$ with excess NH_4SCN in aqueous DMF afforded *trans*-$[Ru(dpp)(NCS)_2]$ (**1e**) as a dark solid in 86% yield. The thiocyanate complex is not soluble in common solvents, and its ^1H NMR spectrum in DMSO-d_6 is different from that of the chloride precursor. The coordination of thiocyanate is confirmed by Fourier transform infrared (FTIR) that shows a strong stretching vibration at 2105 cm^{-1}. Although S-bonded thiocyanate appears at higher wavenumbers than the N-bonded analogue, the difference is typically less than 10 cm^{-1}. Freedman and co-workers observed 2109 and 2099 cm^{-1} for a pair of linkage isomers, $[Ru(p\text{-cymene})(bpy)(SCN)]^+$ and $[Ru(p\text{-cymene})(bpy)(NCS)]^+$, respectively.[7] Pakkanen and co-workers found a strong band at 2116 cm^{-1} assignable to SCN^- stretching for the S-bonded *trans*-thiocyanate complex $[Ru(bpy)(CO)_2(SCN)_2]$.[8] Thus, the bonding mode of thiocyanate to Ru^{II} in complex **1e** remains unclear. Chloride abstraction by $AgBF_4$ in CH_3CN, followed by counterion exchange with NH_4PF_6, gave *trans*-$[Ru(dpp)(CH_3CN)_2](PF_6)_2$ (**1f**) in 96% yield. The complex was characterized by its ^1H NMR spectrum in acetone-d_6. Elemental analysis was not satisfactory probably because of silver salt contamination, but attempts to purify the material by column chromatography resulted in decomposition. No molecular mass peak corresponding to $[Ru(dpp)(CH_3CN)_2]^+$ was detected in the MALDI-TOF spectrum, but two fragments, $[Ru(dpp)(PF_6)]^+$ and $[Ru(dpp)]^+$, were found at m/z 580.4 and 436.3, respectively.

Following a literature method for the synthesis of *trans*-$[Ru(tpy)(2\text{-pyridone})_2(H_2O)]$,[9] treatment of *trans*-$[Ru^{II}(dpp)Cl_2]$ with 2-hydroxypyridine in aqueous EtOH, followed by the addition of NaOH, produced *trans*-$[Ru(dpp)(2\text{-pyridone})_2]$ (**1g**) in 82% yield. All of the dpp protons resonate at lower field (10.24–7.82 ppm), while the pyridone signals appear at higher field (6.67–5.51 ppm).

Attempts to prepare *trans*-$[Ru(dpp)(PPh_3)_2]^{2+}$ (**1h**) by the reaction of *trans*-$[Ru^{II}(dpp)Cl_2]$ with triphenylphosphine (PPh_3) were not successful. The PPh_3 complex was instead synthesized by the treatment of *trans*-$[Ru(dpp)(CH_3CN)_2]^{2+}$ with PPh_3 in a solvent mixture of acetone/EtOH at reflux. However, the reaction was slow and, using 70 equiv of PPh_3, only 75% conversion was observed after 2 days at reflux.

The crystal structure of $[Ru(dpp)(4\text{-}NMe_2py)_2](PF_6)_2$ (**1a**) revealed dpp as a tetradentate ligand,[5] but the binding angles were significantly distorted. The exterior N–Ru–N angle of 125.6° is more than 35° greater than the 90° ideal, indicating weak bonding by the distal pyridines. The fact that dpp binds to a metal in a tetradentate fashion in the presence of a large excess of pyridines in refluxing aqueous EtOH supports the importance of the chelation effect for dpp. However, in the presence of a stronger chelating ligand, such as bpy or tpy, ligand substitution for the weakly bonded distal pyridine on dpp is observed, forcing dpp to bind in a tridentate fashion. A small amount of $[Ru(dpp\text{-}N,N',N'')_2]^{2+}$ (**2**; Scheme 3) was isolated as a byproduct during the one-pot synthesis of **1a**–**1c**[5] and this same material is formed when $[RuCl_3{\cdot}3H_2O]$ is treated with excess dpp in refluxing aqueous EtOH. The ability of dpp to act as a tridentate ligand for Ru^{II} was further verified by the reaction of *trans*-$[Ru^{II}(dpp)Cl_2]$ with tpy and bpy, affording $[Ru(dpp\text{-}N,N',N'')(tpy)]^{2+}$ (**3**) and $[Ru(dpp\text{-}N,N',N'')(bpy)Cl]^+$ (**4**) in yields of 79% and 66%, respectively. The MALDI-TOF spectra of complexes **2**–**4** revealed peaks at m/z 915.3, 813.5, and 627.3 corresponding to $[M - PF_6]^+$, repectively. The ^1H NMR spectra of **2**–**4** showed an unsymmetrical pattern for the dpp signals, indicating that it is bound as a tridentate ligand with one of the distal pyridines uncoordinated. An X-ray structure analysis on complex **4** further confirmed that dpp functions as a tridentate ligand with an uncomplexed distal pyridine. We have previously reported 2-(pyrid-2′-yl)-1,10-phenanthroline (mpp) and its homoleptic ruthenium(II) complex $[Ru(mpp)_2]^{2+}$ (**6**).[10]

dx.doi.org/10.1021/ic202648h | *Inorg. Chem.* 2012, 51, 3179–3185

Scheme 2. Synthesis of *trans*-Ru^{II}(dpp-*N,N′,N″,N‴*) Complexes 1a−1h

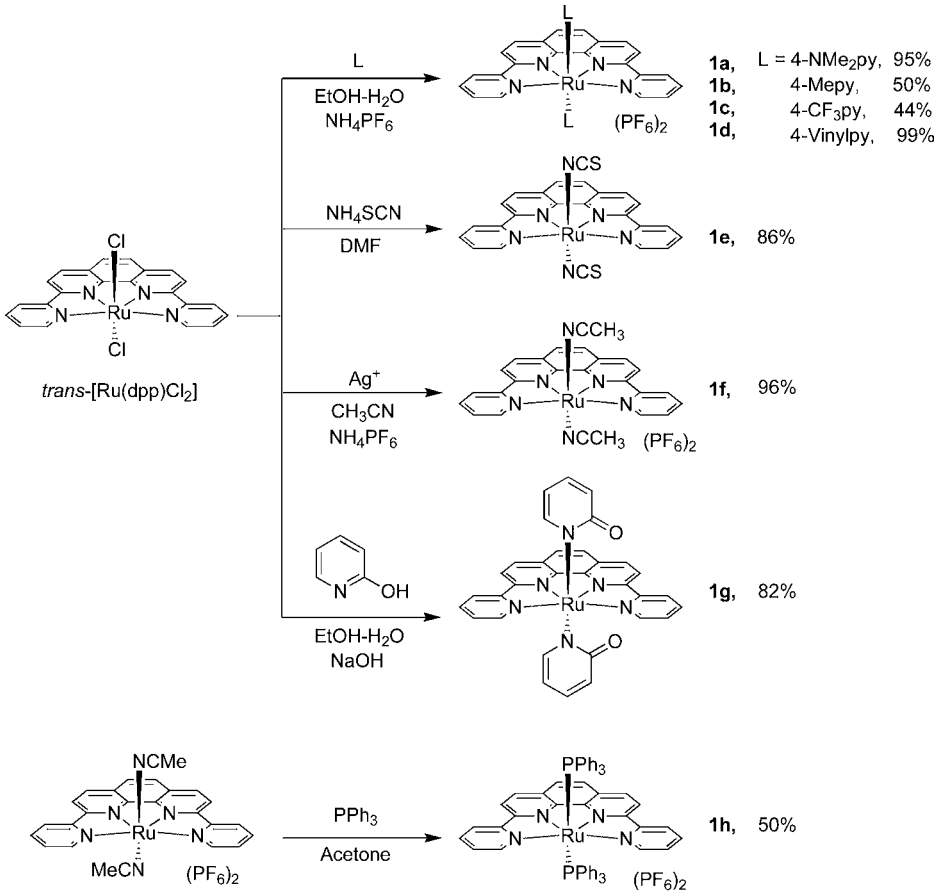

Scheme 3. Synthesis of Tridentate dpp Complexes 2−4

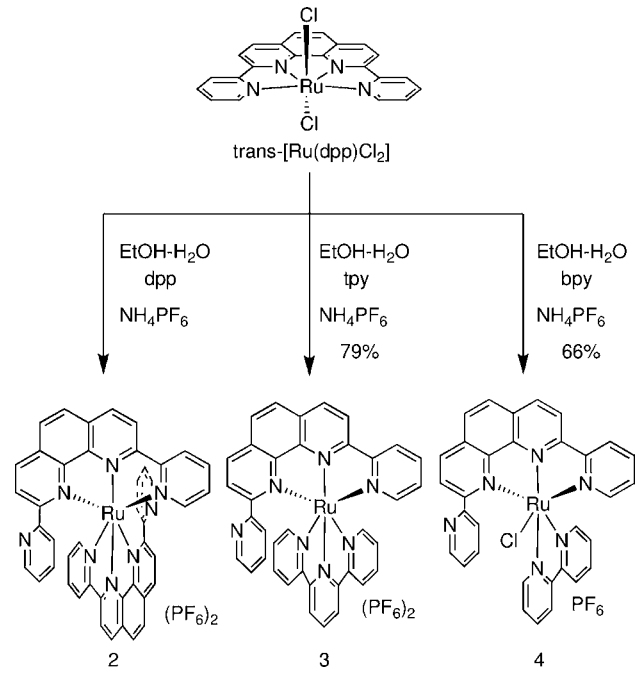

Single crystals of **4**·CH_3CN were obtained by the slow evaporation of a solution of the complex in CH_3CN and toluene. An X-ray analysis revealed its crystal structure (Figure 1), and selected geometric parameters are listed in Table 1. Both the uncoordinated nitrogen N22 and the chloride Cl1 face in

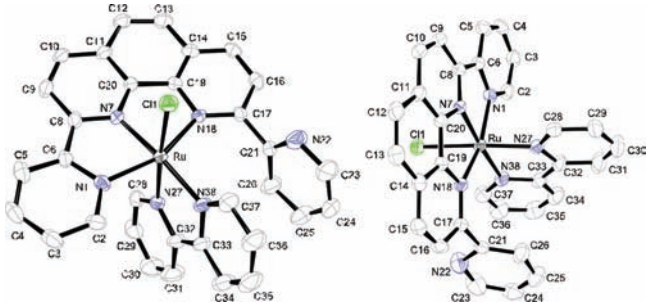

Figure 1. X-ray structure of the cation of **4** (two views) with the atom numbering scheme. Thermal ellipsoids are 40% equiprobability envelopes, with H atoms omitted for clarity.

the same direction below the pyridyl−phenanthroline plane. The central Ru−N7 bond length of 1.953 Å and the other Ru−N distances ranging from 2.026 to 2.132 Å as well as the Ru−Cl bond length of 2.413 Å are typical for [Ru^{II}(tpy)(bpy)Cl]$^+$-type complexes.[11,12] However, the presence of the uncoordinated pyridine ring somewhat distorts the geometry of the Ru^{II} coordination sphere. This uncoordinated pyridine lies parallel to the bpy main plane, showing $\pi-\pi$ interactions evidenced by the nonbonding distances of 3.24 and 3.90 Å for C21−N38 and C24−C35, respectively. The influence of the $\pi-\pi$ interactions is demonstrated by the bond angle of 174.2° for N7−Ru−N38. The larger bond angle of 106.1° for N18−Ru−N38 compared to 95.8° for N1−Ru−N38 indicates that the bpy ligand is forced to move away from the uncoordinated pyridine ring and the Ru−N18 bond (2.13 Å) is longer than 2.07 Å for Ru−N1.

dx.doi.org/10.1021/ic202648h | *Inorg. Chem.* 2012, 51, 3179−3185

Table 1. Selected Geometric Parameters for 4·CH_3CN[a]

Bond Lengths (Å)			
Ru−N1	2.068(4)	Ru−N7	1.953(4)
Ru−N18	2.132(4)	Ru−N27	2.026(4)
Ru−N38	2.076(4)	Ru−Cl1	2.4136(12)
C21−N38	3.24	C24−C35	3.90
Bond Angles (deg)			
N7−Ru−N1	78.43(15)	N7−Ru−N18	79.62(14)
N27−Ru−N38	78.71(16)	N1−Ru−N38	95.81(15)
N38−Ru−N18	106.13(14)	N27−Ru−N1	88.21(14)
N27−Ru−N18	95.16(14)	N7−Ru−N38	174.20(14)
Torsion Angles (deg)			
N1−C6−C8−N7	5.2(6)	C5−C6−C8−C9	5.8(8)
N27−C32−C33−N38	−2.5(6)	C31−C32−C33−C34	−2.8(9)
N18−C17−C21−N22	−104.2(5)	N18−C17−C21−C26	81.5(6)

[a]Goodness of fit on F^2 = 1.039; final R indices for $I > 4(I)$, R1 = 0.0408 and wR2 = 0.1086.

The uncoordinated pyridine is not perpendicular to the pyridyl−phenanthroline plane, as evidenced by torsion angles of 81.5° and −104.2° for N18−C17−C21−C26 and N18−C17−C21−N22 that deviate significantly from 90°. It is interesting that the uncoordinated nitrogen N22 is positioned syn to the chloride. The location of N22 was determined by alternately refining the N atom at both ortho positions (22 and 26). When the N atom is refined in position 22, the U_{eq} values of N22 and C26 are essentially identical and very similar to the U_{eq} values of C23 to C25. When the N atom is refined in position 26, the U_{eq} value of C22 drops by 30% and the U_{eq} value of N26 rises by 40%, indicating quite clearly that the N atom is in position 22 for this particular crystal. The reason for the absence of the anti conformer is not clear. We have carried out Chem3D calculations for the syn and anti isomers and found no significant differences in their steric energy. Semiempirical quantum calculations using the *PM6* program[13] showed similar heats of formation for both the syn and anti isomers.

Electronic Absorption and Emission Properties. In our earlier communication, we observed that the metal-to-ligand charge transfer (MLCT) absorbance of complexes **1a**−**1c** (Table 2) could be tuned by the 4 substituent on the axial monodentate pyridines.[5] Four absorption maxima were observed in the visible region and shifted to lower energy as the substituent was changed from electron-withdrawing (CF_3) to electron-donating (NMe_2). The low-energy MLCT band at 541 nm for VP complex **1d** resembles the 544 nm band found for its 4-methylpyridine analogue (**1b**).

Unlike complexes **1a**−**1d**, where a 4-substituted pyridine occupies the axial sites, the CH_3CN (**1f**) and PPh_3 (**1h**) complexes show blue-shifted absorptions at 474 and 488 nm, respectively (Figure 2). This difference in behavior depends upon the pyridine functioning as both a σ donor and a π acceptor, whereas PPh_3 and CH_3CN act only as σ donors. Although the 2-pyridone complex (**1g**) geometry is similar to that of **1a**−**1f** and **1h**, it exhibits two broad absorption maxima at 530 and 645 nm that extend beyond 800 nm because of a combination of the π-acceptor strength and the enhanced σ-donor ability of the anionic ligand (Figure 2).

The previously prepared complex **6** absorbs at 498 nm in CH_3CN.[10] Displaying a similar absorption profile, the dpp complex **2** has a weaker absorbance than the mpp complex **6**. A broad absorption band with several shoulders and a peak at 499 and 503 nm was observed for the homoleptic complexes **6** and **2**, respectively (Figure 3). In **2**, the presence of an uncoordinated pyridine on each dpp ligand lowers the absorption energy by about 4 nm. It is interesting that the heteroleptic complex **3**, with one tpy ligand and one tridentate dpp ligand, shows two peaks at 474 and 493 nm, which are close to absorption maxima of the corresponding homoleptic complexes **5** and **2**, respectively. As expected, the heteroleptic chloro complex **4** absorbs at low energy and its absorbance is much broader than the complexes **2**, **3**, and **6**.

Table 2. Electronic Absorption Data for Ruthenium(II) Complexes 1−6[a]

complex	auxiliary ligands	λ_{max} (log ε)
1a	4-NMe_2py	225 (4.46), 259 (4.71), 281 (4.87), 313 (4.78), 445 (3.61), 479 (3.67), 514 (3.71), 580 (3.81)
1b	4-Mepy	226 (sh, 4.53), 241 (4.64), 279 (4.81), 315 (4.66), 411 (3.70), 456 (3.58), 487 (3.74), 544 (3.91)
1c	4-CF_3py	224 (4.47), 241 (4.60), 277 (4.77), 307 (4.51), 338 (4.56), 372 (4.21), 437 (3.56), 469 (3.74), 516 (3.89)
1d	VP	252 (4.70), 280 (4.72), 315 (4.47), 341 (4.47), 370 (4.22), 455 (3.53), 489 (3.69), 541 (3.82)
1e	SCN^-	insoluble
1f	CH_3CN	234 (4.40), 277 (4.68), 302 (4.33), 334 (4.44), 488 (3.71)
1g	2-pyridone	275 (4.51), 285 (4.54), 319 (4.42), 530 (3.74), 645 (3.61)
1h	PPh_3	233 (4.71), 276 (4.81), 338 (4.41), 474 (3.69)
2	dpp	241 (4.58), 302 (4.58), 342 (4.39), 503 (3.90)
3	tpy	242 (4.59), 263 (4.53), 307 (4.68), 474 (3.98), 493 (3.97)
4	bpy and Cl^-	243 (4.57), 297 (4.58), 347 (4.22), 503 (3.83), 560 (3.74)
5		271 (4.40), 309 (4.63), 476 (3.99)
6		296 (4.84), 325 (4.54), 339 (4.64), 499 (4.15)

[a]Recorded in 5 × 10^{-5} M CH_2Cl_2; wavelengths are given in nm and extinction coefficients in M^{-1} cm^{-1}.

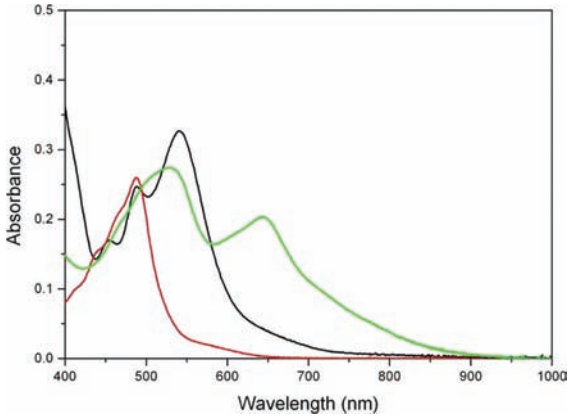

Figure 2. Electronic absorption spectra of **1d** (black), **1f** (red), and **1g** (green) recorded in CH_2Cl_2 (5 × 10^{-5} M).

The Ru(dpp) complexes, regardless of whether the dpp functions as a tetradentate ligand (**1a**−**1h**) or as a tridentate ligand (**2**−**4**), do not emit or emit very weakly because of the strain impacted by two or three fused five-membered chelate rings. The chloro complex **4** emits at 790 nm with a large Stokes shift when excited at 590 nm. It is interesting to find that the pyridone complex **1g** emits at 721 nm when excited at its low-energy (645 nm) or next-higher-energy MLCT absorbance (530 nm). The corresponding Stokes shifts are 76 and 191 nm, respectively. A large Stokes shift in this case does not necessarily

dx.doi.org/10.1021/ic202648h | *Inorg. Chem.* 2012, 51, 3179−3185

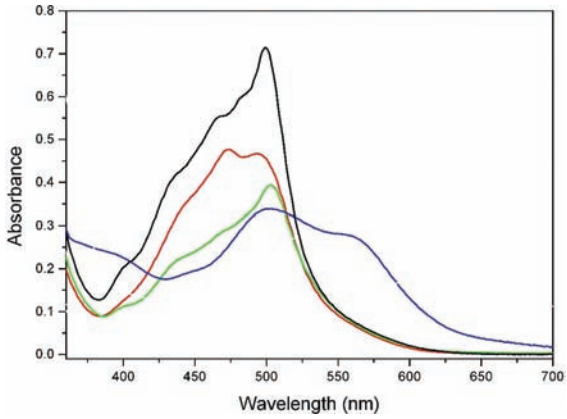

Figure 3. Electronic absorption spectra of **2** (green), **3** (red), **4** (blue), and **6** (black).

represent a large distortion of the excited state because the absorption is a singlet−singlet process and the emission is triplet to ground-state singlet. A large singlet−triplet gap can account for the large Stokes shift without the requirement of significant distortion. It is not clear at this stage if the uncoordinated pyridine on dpp in complexes **2**−**4** is playing a role in the excited state of the complex.

Electrochemistry. The redox potentials for complexes **1**−**6** were measured by cyclic voltammetry (CV) using a glassy carbon working electrode. The data are tabulated in Table 3, and potentials are referenced to a saturated calomel electrode (SCE).

Table 3. CV Data for Ruthenium(II) Complexes 1−6[a]

compound	auxiliary ligands	$E_{1/2}^{ox}$ (ΔE)	$E_{1/2}^{red}$ (ΔE)
1a[b]	4-NMe_2py	0.91 (77)	−0.93 (98), −1.33 (116)
1b[b]	4-Mepy	1.24 (89)	−0.87 (70), −1.26 (99)
1c[b]	4-CF_3py	1.39 (100)	−0.82 (82), −1.20 (96)
1d	VP	1.23 (228)	−1.03 (75), −1.58 (119)
1e	SCN^-	insoluble	
1f	CH_3CN	1.31 (228)	−1.13 (72), −1.74[ir]
1g	2-pyridone	insoluble	
1h	PPh_3	1.55 (93)	−0.93[ir], −1.04 (163), −1.59 (102)
2	dpp	1.27 (137)	−1.15 (83), −1.40 (83), −1.87[ir]
3	tpy	1.36 (184)	−1.12 (70), −1.52 (83), −1.80 (90)
4	bpy and Cl^-	0.82 (79)	−1.24 (76), −1.58 (90), −1.82[ir]
5		1.22 (102)	−1.33 (90), −1.55 (78)
6		1.36 (101)	−1.06 (63), −1.29 (76), −1.75 (88)

[a]Measured with a glassy carbon electrode at 100 mV s^{-1} in CH_3CN containing 0.1 M $N(n\text{-}Bu)_4PF_6$ and reported in V relative to SCE; $E_{1/2} = (E_{pa} + E_{pc})/2$ in V and $\Delta E = (E_{pa} - E_{pc})$ in mV. [b]Reference 5.

In an earlier communication, we reported complexes **1a**−**1c** including their electrochemical data measured in CH_2Cl_2.[5] The oxidation corresponds to the removal of an electron from the metal, while the first reduction is attributable to the addition of an electron to the LUMO, likely to be associated with the most electron-deficient ligand dpp. Pyridine ligands are best known for their σ-donor ability because of the lone pair of electrons on the N atom and their π-acceptor character associated with the π system. We found that the ruthenium-centered oxidation is quite sensitive to the overall ligand field strength of the axial pyridines bearing different substituents at the 4 position. The half-wave potential of the complexes correlates well with the σ-donor ability of the pyridine, which is a function of the substituent on pyridine. The electron-donating NMe_2 group causes a less positive oxidation potential compared to the electron-withdrawing CF_3. The VP complex **1d** showed an oxidation at 1.23 V, which is very close to that of the 4-methylpyridine analogue. However, the first reduction appears at more negative potential (−1.03 V) compared to −0.87 V for **1b**. It is important to note that the oxidation peak disappears after the reduction scan, which may indicate decomposition of the complex on the electrode surface. Oxidation of the acetonitrile complex **1f** occurs at 1.31 V vs SCE, which is comparable to that of the CF_3 complex **1c**. However, the first reduction for **1f** at −1.13 V is more negative than −0.82 V for **1c**. Oxidation of the PPh_3 complex **1h** at 1.55 V is the most positive potential measured for the trans series complexes (**1a**−**1h**).

The first oxidations/reductions of the homoleptic complexes **5** and **6** appear at 1.22/−1.33 and 1.36/−1.06 V vs SCE, respectively, reflecting more positive oxidation and less negative reduction for the more π-extended ligand system. The corresponding redox values of 1.27/−1.15 and 1.36/−1.12 V vs SCE for **2** and **3** are consistent with the existence of one or two dpp as a more π-extended ligand than tpy. However, the correlation does not apply when one compares **2** and **6**. As demonstrated by the crystal structure of **4**, the uncoordinated pyridine is twisted by about 81.5° relative to the mpp plane. The less positive and more negative potentials for the homoleptic complex **2** compared to **6** reflect the influence of the two uncoordinated pyridines. The heteroleptic complex **3** bearing one uncoordinated pyridine oxidizes at slightly higher potential than **2**, which bears two uncoordinated pyridines, but their first reduction potentials are nearly the same. For the heteroleptic complexes **3** and **4**, the first reduction is dpp-based and the second reduction is attributed to a tpy/bpy-based process. As expected, the presence of an anionic ligand stabilizes the higher oxidation state of ruthenium and lowers the oxidation potential by more than 0.4 V. The coordinated chloride, being cis to the pyridyl−phenanthroline plane, also makes the dpp-based reduction more negative.

■ CONCLUSION

The complex *trans*-$[Ru^{II}(dpp)Cl_2]$ serves as a convenient reagent for the preparation of a series of *trans*-Ru(dpp) complexes **1a**−**1h**, where dpp is a planar tetradentate ligand. Axial ligands exert significant effects on the absorption and redox properties of the complexes. It is of interest to find that *trans*-$[Ru^{II}(dpp)Cl_2]$ functions as the source for a tridentate dpp complex of ruthenium. The reaction of *trans*-$[Ru^{II}(dpp)Cl_2]$ with dpp, tpy, or bpy produces ruthenium(II) complexes (**2**−**4**), where one of the distal pyridines on dpp was replaced by the other polydentate ligand. The X-ray crystal structure of $[Ru(dpp\text{-}N,N',N''')(bpy)Cl](PF_6)\cdot CH_3CN$ revealed that the uncoordinated pyridine experiences π−π interaction with bpy and the uncoordinated N atom is positioned cis to the chloride. The uncoordinated pyridine, covalently bound to a tridentate ligand, tends to lower the oxidation potential of the ruthenium(II) complex, slightly influences the reduction potentials, and red-shifts the absorption maxima by a few nanometers.

■ EXPERIMENTAL SECTION

The ligand dpp,[5] $[Ru(DMSO)_4Cl_2]$,[14] $[Ru(tpy)_2](PF_6)_2$ (**5**),[12] and $[Ru(mpp)_2](PF_6)_2$ (**6**)[10] were prepared according to literature methods. Complexes **1a** and **1b** were reported previously.[5] $[RuCl_3\cdot 3H_2O]$, 2-hydroxypyridine, PPh_3, 4-(trifluoromethyl)pyridine, bpy, tpy, and all solvents were commercially available and were used

dx.doi.org/10.1021/ic202648h | Inorg. Chem. 2012, 51, 3179−3185

without further purification. The alumina used for chromatography was neutral Brockman grade I. All reactions were carried out under air, and yields were calculated from a single run and not optimized. ^{1}H NMR spectra were recorded with a JEOL ECX-400 or a ECA-500 spectrometer operating at 400 and 500 MHz, respectively. The chemical shifts were reported in parts per million (ppm) and were referenced to the solvent residue peaks, which were referenced to tetramethylsilane. The electronic absorption spectra were recorded on a Varian Cary 50 UV−vis spectrophotometer, and all spectra were corrected for the background spectrum of the solvent. Luminescence measurements were performed on a Perkin-Elmer LS-50B luminescence spectrometer at room temperature. CV measurements were carried out on a Bioanalysis BAS Epsilon Electroanalytical System. The CV experiments were performed in a one-compartment cell equipped with a glassy carbon working electrode, a SCE, and a platinum wire auxiliary electrode. Attenuated total reflection (ATR) IR spectra were measured on a Thermo Nicolet AVATAR 370 RT-IR spectrometer. Mass spectra were obtained on a ABI Voyager DE-STR (MALDI-TOF) and a Thermo Finnigan LCQ DecaXP Plus with Surveyor liquid chromatography−mass spectrometry (LC−MS). Elemental analyses were carried out by QTI (Whitehouse, NJ).

***trans*-[Ru^{II}(dpp)Cl$_2$].** A solution of [Ru(DMSO)$_4$Cl$_2$] (89 mg, 0.18 mmol) and dpp (61 mg, 0.18 mmol) in $CHCl_3$ (7 mL) was refluxed for 22 h. The precipitate was collected, washed with CH_2Cl_2 and acetone, and dried to afford the desired complex (82 mg, 89%): ^{1}H NMR (400 MHz, DMSO-d_6) δ 9.95 (d, J = 4.58 Hz, 2H), 8.84 (d, J = 8.70 Hz, 2H), 8.79 (d, J = 7.79 Hz, 2H), 8.37 (d, J = 8.70 Hz, 2H), 8.30 (s, 2H), 8.28 (dt, J = 1.37 and 7.79 Hz, 2H), 7.98 (ddd, J = 1.15, 5.27, and 7.56 Hz, 2H); MS (MALDI-TOF) m/z 506.3 [M]$^+$, 471.3 [M − Cl]$^+$, 436.4 [M − 2Cl]$^+$; FTIR (ATR, cm^{-1}) ν 1600, 1453, 1407, 1361, 1276, 1226. Anal. Calcd for $C_{22}H_{14}N_4Cl_2Ru\,H_2O$: C, 50.38; H, 3.05; N, 10.68. Found: C, 50.69; H, 2.93; N, 10.60.

***trans*-[Ru(dpp)(4-CF$_3$-py)$_2$](PF$_6$)$_2$ (1c).**[5] A mixture of *trans*-[Ru^{II}(dpp)Cl$_2$] (57 mg, 0.11 mmol) and 4-(trifluoromethyl)pyridine (250 mg, 1.70 mmol) in EtOH/H_2O (15:5 mL) was refluxed overnight. The reaction mixture was concentrated to about 5 mL, and NH_4PF_6 (162 mg, 1.0 mmol) was added. The precipitate was collected and purified by chromatography on alumina, eluting with CH_2Cl_2/acetone followed by acetone/H_2O to afford complex **1c** (48 mg, 44%): ^{1}H NMR (400 MHz, acetone-d_6) δ 10.31 (d, J = 4.6 Hz, 2H), 8.89 (AB, 4H), 8.67(d, J = 7.8 Hz, 2H), 8.64 (s, 2H), 8.56 (d, J = 6.4 Hz, 4H), 8.39 (dt, J = 1.3 and 7.8 Hz, 2H), 8.15 (dt, J = 1.4 and 7.8 Hz, 2H), 7.36 (d, J = 6.4 Hz, 4H).

A monopyridine complex *trans*-[Ru(dpp)(4-CF$_3$-py)Cl](PF$_6$) (18 mg, 22%)[5] was also obtained from early fractions of the alumina column by eluting with acetone: ^{1}H NMR (acetone-d_6) δ 10.07 (d, J = 4.2 and 1.5 Hz, 2H), 8.82 (d, J = 8.4 Hz, 2H), 8.71 (d, J = 7.8 Hz, 2H), 8.60 (d, J = 8.7 Hz, 2H), 8.49 (d, J = 6.9 Hz, 2H), 8.43 (s, 2H), 8.34 (dt, J = 7.8 and 1.5 Hz, 2H), 8.05 (m, 2H), 7.27 (d, J = 7.2 Hz, 2H); IR (ATR, cm^{-1}) 1603 (vw), 1419 (vw), 1332 (m), 1179 (w), 1142 (w), 1092 (w), 1056 (vw), 838 (vs), 773 (m), 730 (m), 680 (vw); MS (LC−MS, acetone) m/z 617.9 [M − PF$_6$]$^+$, 763.7 [M]$^+$.

[Ru(dpp)(VP)$_2$](PF$_6$)$_2$ (1d). A mixture of *trans*-[Ru^{II}(dpp)Cl$_2$] (34 mg, 0.066 mmol), VP (393 mg, 3.74 mmol), EtOH (10 mL), and H_2O (3 mL) was heated at reflux for 2 days. The volatile material was evaporated at reduced pressure. NH_4PF_6 (168 mg, 1.0 mmol) was added to produce a precipitate that was collected and washed with H_2O. Recrystallization with acetone/H_2O afforded the complex (64 mg, 100%): ^{1}H NMR (400 MHz, acetone-d_6) δ 10.29 (dd, J = 0.92 and 5.50 Hz, 2H), 8.89 (d, J = 8.70 Hz, 2H), 8.82 (d, J = 8.70 Hz, 2H), 8.68 (d, J = 7.79 Hz, 2H), 8.61 (s, 2H), 8.38 (dt, J = 1.83 and 7.79 Hz, 2H), 8.15 (ddd, J = 1.37, 5.04, and 7.79 Hz, 2H), 8.05 (dd, J = 1.37 and 5.50 Hz, 4H), 7.08 (dd, J = 1.37 and 5.04 Hz, 4H), 6.48 (dd, J = 10.99 and 17.86 Hz, 2H), 5.90 (d, J = 17.86 Hz, 2H), 5.44 (d, J = 10.99 Hz, 2H). Anal. Calcd for $C_{36}H_{28}F_{12}N_6P_2Ru\cdot{}^1/_2H_2O$: C, 45.77; H, 3.09; N, 8.90. Found: C, 45.76; H, 3.11; N, 8.68.

***trans*-[Ru(dpp)(NCS)$_2$] (1e).** To a solution of *trans*-[Ru^{II}(dpp)Cl$_2$] (31 mg, 0.060 mmol) in DMF (5 mL) was added ammonium thiocyanate (366 mg, 4.8 mmol) in H_2O (2.5 mL). The mixture was refluxed for 18 h. The black precipitate was collected, washed with H_2O, and dried to give a dark solid (28.8 mg, 86%): ^{1}H NMR (DMSO-d_6) δ 9.92 (d, J = 4.8 Hz, 2H), 8.94 (d, J = 8.4 Hz, 2H), 8.86 (d, J = 7.5 Hz, 2H), 8.62 (d, J = 9.0 Hz, 2H), 8.37 (m, 4H), 8.04 (t, J = 6.3 Hz, 2H); FTIR (ATR, cm^{-1}) ν 2105 (SCN), 1601, 1454, 1444, 1363, 1282. Anal. Calcd for $C_{24}H_{14}N_6RuS_2$: C, 52.26; H, 2.56; N, 15.24. Found: C, 51.78; H, 2.43; N, 14.89.

***trans*-[Ru(dpp)(2-pyridone)$_2$] (1g).** A mixture of *trans*-[Ru^{II}(dpp)Cl$_2$] (30 mg, 0.059 mmol) and 2-hydroxypyridine (40 mg, 0.42 mmol) in EtOH/H_2O (15:5 mL) was heated at reflux for 22 h. NaOH (93 mg, 2.3 mmol) was added and reflux was continued overnight. The solvents were evaporated, and H_2O (5 mL) was added to the residue. The solid was collected, washed with H_2O and acetone, and dried (30 mg, 82%): ^{1}H NMR (400 MHz, DMSO-d_6) δ 10.24 (d, J = 4.58 Hz, 2H), 8.45 (d, J = 8.70 Hz, 2H), 8.28 (d, J = 7.79 Hz, 2H), 8.27 (d, J = 8.93 Hz, 2H), 8.23 (s, 2H), 8.01 (dt, J = 1.83 and 7.79 Hz, 2H), 7.82 (ddd, J = 1.37, 5.50, and 7.33 Hz, 2H), 6.77 (dd, J = 1.83 and 5.95 Hz, 2H), 6.65 (ddd, J = 2.06, 6.64, and 8.70 Hz, 2H), 5.58 (dd, J = 0.92 and 8.70 Hz, 2H), 5.51 (dt, J = 1.37 and 6.41 Hz, 2H). Anal. Calcd for $C_{32}H_{22}N_6O_2Ru\cdot 2H_2O$: C, 58.26; H, 3.97; N, 12.74. Found: C, 58.67; H, 3.91; N, 12.42.

***trans*-[Ru(dpp)(CH$_3$CN)$_2$](PF$_6$)$_2$ (1f).** A mixture of *trans*-[Ru^{II}(dpp)Cl$_2$] (43.6 mg, 0.086 mmol) and $AgBF_4$ (50 mg, 0.26 mmol) in CH_3CN (5 mL) was heated at reflux overnight. The resulting mixture was passed through a short column of alumina, and the first, light-brown band was collected to give a brown solid, which was dissolved in CH_3CN, to which was added NH_4PF_6 (81 mg) in H_2O (1 mL). Evaporation of CH_3CN afforded **1f** (57 mg, 96%): ^{1}H NMR (400 MHz, acetone-d_6) δ 9.89 (d, J = 4.58 Hz, 2H), 8.94 (d, J = 8.70 Hz, 2H), 8.85 (m, 2H), 8.85 (d, J = 8.70 Hz, 2H), 8.49 (dt, 1.83, 7.79 Hz, 2H), 8.46 (s, 2H), 8.07 (ddd, J = 1.37, 5.50, and 7.79 Hz, 2H). MS (MALDI-TOF): m/z 580.4 [Ru(dpp)(PF$_6$)]$^+$, 436.3 [Ru(dpp)]$^+$.

***trans*-[Ru(dpp)(PPh$_3$)$_2$](PF$_6$)$_2$ (1h).** A mixture of *trans*-[Ru^{II}(dpp)-(CH$_3$CN)$_2$](PF$_6$)$_2$ (8.5 mg, 0.010 mmol) and PPh_3 (180 mg, 0.69 mmol) in an acetone/EtOH mixture (5:5 mL) was heated at reflux overnight. The solvents were evaporated, and the residue, dissolved in acetone (0.5 mL), was added dropwise to ether (5 mL). The precipitate was collected, washed with ether, and dried to give a light-brown solid (10 mg), which was a mixture of the starting materials and the PPh_3 complex in a 1:2 ratio. The mixture, along with **1f** (9.9 mg, 0.011 mmol), was refluxed with PPh_3 (195 mg, 0.74 mmol) for 2 days. Solvents were removed, and the residue in minimum amount of acetone was added to the ether to afford a precipitate. The solid was collected, washed with ether, and dried (13 mg, 50%): ^{1}H NMR (400 MHz, acetone-d_6) δ 10.42 (d, J = 5.50 Hz, 2H), 8.60 (d, J = 8.70 Hz, 2H), 8.43 (s, 2H), 8.21 (d, J = 8.70 Hz, 2H), 8.08 (m, 4H), 7.83 (dt, J = 3.66 and 5.50 Hz, 2H), 7.34 (t, J = 7.56 Hz, 6H, *PPh*$_3$), 7.09 (m, 12H, *PPh*$_3$), 6.59 (m, 12H, *PPh*$_3$); ^{13}P NMR (162 Hz, acetone-d_6) δ 30.55 (s, *PPh*$_3$). Anal. Calcd for $C_{58}H_{44}F_{12}N_4P_4Ru\,H_2O$: C, 54.94; H, 3.66; N, 4.42. Found: C, 54.98; H, 3.31; N, 4.47.

[Ru(dpp-*N*,*N*′,*N*″)$_2$](PF$_6$)$_2$ (2).[5] The complex **2** was obtained as a byproduct in the previously reported[5] one-pot syntheses of complexes **1a**−**1c**: ^{1}H NMR (400 MHz, acetone-d_6) δ 9.15 (d, J = 9.16 Hz, 2H), 8.94 (d, J = 8.59 Hz, 2H), 8.84 (d, J = 7.45 Hz, 2H), 8.79 (d, J = 8.02 Hz, 2H), 8.50 (AB, 4H), 8.00 (dt, J = 1.72 and 7.73 Hz, 2H), 7.69 (d, J = 4.58 Hz, 2H), 7.58 (d, J = 8.02 Hz, 2H), 7.12 (ddd, J = 1.72, 5.73, and 7.45 Hz, 2H), 7.09 (dt, J = 1.72 and 7.73 Hz, 2H), 6.86 (m, 4H), 6.36 (d, J = 7.45 Hz, 2H); MS (MALDI-TOF, no matrix) m/z 915.3 [M − PF$_6$]$^+$, 769.3 [M − 2PF$_6$]$^+$.

[Ru(dpp-*N*,*N*″,*N*″)(tpy)](PF$_6$)$_2$ (3). A suspension of *trans*-[Ru^{II}(dpp)Cl$_2$] (43 mg, 0.085 mmol), tpy (26.3 mg, 0.113 mmol), EtOH (10 mL), and H_2O (3 mL) was refluxed for 2 days to give a red solution. NH_4PF_6 (162 mg, 1.0 mmol) was added to produce a precipitate, which was collected and purified by chromatography first on alumina and then on silica gel to provide a red solid (44 mg, 54%): ^{1}H NMR (400 MHz, acetone-d_6) δ 9.28 (d, J = 8.70 Hz, 1H), 9.16 (d, J = 8.70 Hz, 1H), 8.86 (d, J = 7.79 Hz, 1H), 8.85 (d, J = 8.24 Hz, 1H), 8.79 (d, J = 8.24 Hz, 2H), 8.71 (d, J = 9.16 Hz, 1H), 8.71 (d, J = 7.79 Hz, 2H), 8.58 (d, J = 9.16 Hz, 1H), 8.37 (d, J = 8.02 Hz, 1H), 8.23 (m, 1H), 8.06 (dt, J = 1.83 and 7.79 Hz, 2H), 8.02 (dt, J = 1.83 and 7.79 Hz, 1H), 7.66 (d, J = 8.70 Hz, 1H), 7.63 (d, J = 1.83 and 7.79 Hz, 1H), 7.61 (dt, J = 0.92 and 4.58 Hz, 2H), 7.28 (m, H + H), 7.21 (ddd,

dx.doi.org/10.1021/ic202648h | *Inorg. Chem.* 2012, 51, 3179−3185

J = 1.37, 5.50, and 7.33 Hz, 2H), 6.92 (td, J = 0.92 and 5.04 Hz, 1H), 6.63 (td, J = 0.92 and 7.79 Hz, 1H); MS (MALDI-TOF) m/z 813.5 $[M - PF_6]^+$, 669.5 $[M - 2PF_6]^+$. Anal. Calcd for $C_{37}H_{25}N_7F_{12}P_2Ru$: C, 46.36; H, 2.63; N, 10.23. Found: C, 46.44; H, 2.57; N, 9.77.

[Ru(dpp-*N*,*N*′,*N*″)(bpy)Cl](PF$_6$) (4). A mixture of *trans*-$[Ru^{II}(dpp)Cl_2]$ (40 mg, 0.079 mmol), bpy (38 mg, 0.24 mmol), EtOH (10 mL), and H_2O (3 mL) was heated at reflux for 2 days to give a red solution. NH_4PF_6 (162 mg, 1.0 mmol) was added to produce a precipitate that was collected and purified by chromatography first on alumina and then on silica gel, eluting with a CH_2Cl_2/acetone mixture. Complex **4** was obtained as a light-brown solid (32 mg, 66%): ^{1}H NMR (400 MHz, acetone-d_6) δ 9.93 (d, J = 5.50 Hz, 1H), 8.99 (d, J = 8.70 Hz, 1H), 8.79 (d, J = 8.70 Hz, 1H), 8.73 (d, J = 8.24 Hz, 1H), 8.72 (d, J = 7.79 Hz, 1H), 8.54 (d, J = 8.24 Hz, 1H), 8.51 (d, J = 8.70 Hz, 1H), 8.46 (d, J = 8.24 Hz, 1H), 8.43 (d, J = 9.16 Hz, 1H), 8.14 (m, 2H), 7.95 (dt, J = 1.37 and 7.79 Hz, 1H), 7.81 (ddd, J = 1.37, 5.78, and 7.56 Hz, 1H), 7.76 (d, J = 7.79 Hz, 1H), 7.76 (d, J = 8.24 Hz, 1H), 7.66 (dt, J = 1.83 and 7.79 Hz, 1H), 7.53 (d, J = 8.24 Hz, 1H), 7.48 (d, J = 5.04 Hz, 1H), 7.33 (ddd, J = 1.37, 5.78, and 7.56 Hz, 1H), 7.12 (m, 2H), 6.95 (ddd, J = 1.37, 5.78, and 7.56 Hz, 1H); MS (MALDI-TOF) m/z 627.3 $[M - PF_6]^+$. Anal. Calcd for $C_{32}H_{22}ClF_6N_6PRu \cdot {}^3/_4CH_2Cl_2$: C, 47.07; H, 2.83; N, 10.06. Found: C, 47.19; H, 2.73; N, 10.26.

X-ray Structure Determination of 4·CH$_3$CN. All measurements were made with a Siemens SMART platform diffractometer equipped with a 4K CCD APEX II detector. A hemisphere of data (1271 frames at a 6 cm detector distance) was collected using a narrow-frame algorithm with scan widths of 0.30° in ω and an exposure time of 35 s/frame. The data were integrated using the Bruker-Nonius *SAINT* program, with the intensities corrected for Lorentz factor, polarization, air absorption, and absorption due to variation in the path length through the detector faceplate. A ψ-scan absorption correction was applied based on the entire data set. Redundant reflections were averaged. Final cell constants were refined using 8155 reflections having $I > 10\sigma(I)$, and these, along with other information pertinent to data collection and refinement, are listed in Table S1 in the Supporting Information. The Laue symmetry was determined to be *mmm*, and from the systematic absences noted, the space group was shown unambiguously to be *Pbca*. Both the anion and the CH_3CN solvent molecule were found to be massively disordered, having three slightly different orientations. This was treated by refinement of ideal rigid bodies at each site, with occupancies estimated based on a comparison of the isotropic displacement parameters involved. No attempt was made to locate or refine the disordered solvent H atoms.

■ ASSOCIATED CONTENT

Ⓢ Supporting Information

X-ray crystallographic data for [Ru(dpp-*N*′,*N*″,*N*‴)(bpy)Cl](PF$_6$)·CH$_3$CN, ^{1}H NMR spectra for complexes *trans*-$[Ru^{II}(dpp)Cl_2]$, *trans*-[Ru(dpp)(4-CF$_3$py)Cl](PF$_6$), **1d**−**1h**, and **2**−**4**, MS spectra (measured and calculated) for *trans*-$[Ru^{II}(dpp)Cl_2]$, **2**−**4**, and the fragment $[Ru(dpp)(PF_6)]^+$ of complex **1f**. This material is available free of charge via the Internet at http://pubs.acs.org.

■ AUTHOR INFORMATION

Corresponding Author

*E-mail: thummel@uh.edu.

Notes

The authors declare no competing financial interest.

■ ACKNOWLEDGMENTS

We thank the Robert A. Welch Foundation (Grant E-621) and the Division of Chemical Sciences, Geosciences, and Biosciences, Office of Basic Energy Sciences, of the U.S. Department of Energy (Grant DE-FG02-07ER15888) for financial support of this work. We also thank Dr. James Korp for assistance with the X-ray determination.

■ REFERENCES

(1) (a) Lehn, J.-M. *Supramolecular Chemistry: Concepts and Perspectives*; Wiley: New York, 1995. (b) Balzani, V.; Bergamini, G.; Marchioni, F.; Ceroni, P. *Coord. Chem. Rev.* **2006**, *250*, 1254−1266. (c) Harriman, A.; Ziessel, R. *Coord. Chem. Rev.* **1997**, *171*, 331−339. (d) Constable, E. C. *Chem. Soc. Rev.* **2007**, *36*, 246−253. (e) Hofmeier, H.; Schubert, U. S. *Chem. Soc. Rev.* **2004**, *33*, 373−399. (f) Winter, A.; Newkome, G. R.; Schubert, U. S. *ChemCatChem* **2011**, *3*, 1384−1406. (g) Constable, E. C. *Adv. Inorg. Chem. Radiochem.* **1986**, *30*, 69−121. (h) Cargill Thompson, A. M.W. *Coord. Chem. Rev.* **1997**, *160*, 1−52.

(2) Juris, A.; Balzani, V.; Belser, P.; von Zelewsky, A. *Helv. Chim. Acta* **1981**, *64*, 2175−2182.

(3) Liu, Y.; Hammitt, R.; Lutterman, D. A.; Thummel, R. P.; Turro, C. *Inorg. Chem.* **2007**, *46*, 6011−6021.

(4) Stewart, D. J.; Fanwick, P. E.; McMillin, D. R. *Inorg. Chem.* **2010**, *49*, 6814−6816.

(5) Zong, R.; Thummel, R. P. *J. Am. Chem. Soc.* **2004**, *126*, 10800−10801.

(6) Zhang, G.; Zong, R.; Tseng, H.-W.; Thummel, R. P. *Inorg. Chem.* **2008**, *47*, 990−998.

(7) Vandenburgh, L.; Buck, M. R.; Freedman, D. A. *Inorg. Chem.* **2008**, *47*, 9134−9136.

(8) Homanen, P.; Haukka, M.; Pakkanen, T. A.; Pursiainen, J.; Laitinen, R. H. *Organometallics* **1996**, *15*, 4081−4084.

(9) Kelson, E. P.; Phengsy, P. P. *Dalton Trans.* **2000**, 4023−4024.

(10) Hung, C.-Y.; Wang, T.-L.; Shi, Z.; Thummel, R. P. *Tetrahedron* **1994**, *50*, 10685−10692.

(11) Hartshorn, C. M.; Maxwell, K. A.; White, P. S.; DeSimone, J. M.; Meyer, T. J. *Inorg. Chem.* **2001**, *40*, 601−606.

(12) Tseng, T.-W.; Zong, R.; Muckerman, J. T.; Thummel, R. *Inorg. Chem.* **2008**, *47*, 11763−11773.

(13) Stewart, J. J. P. *J. Mol. Model.* **2007**, *13*, 1173−1213.

(14) Evans., I. P.; Spencer, A.; Wilkinson, G. *J. Chem. Soc., Dalton Trans.* **1973**, 204−209.

■ NOTE ADDED AFTER ASAP PUBLICATION

Due to a production error, this paper was published on the Web on February 10, 2012, with reference 8 being incorrect. The corrected version was reposted on February 16, 2012.